32 Nienhaus, F., Schuiling, M., Gliem, G., Schinzer, U., and Spittel, A., Investigations on the etiology of the lethal disease of coconut palm in Tanzania. Z. PflKrankh. PflSchutz *89* (1982) 185–193.
33 Nienhaus, F., and Sikora, R.A., Mycoplasmas, Spiroplasmas and Rickettsia-like organisms as plant pathogens. A. Rev. Phytopath. *17* (1979) 37–58.
34 Nienhaus, F., and Yarwood, C.E., Transmission of virus from oak leaves fractionated with sephadex. Phytopathology *62* (1972) 313–315.
35 Parameswaran, N., Occurrence of mycoplasma-like bodies in phloem cells of beech trees affected by 'bark necrosis'. Ann. Sci. Forest. *37* (1980) 371–372.
36 Plumb, R.T., and Thresh, J.M., Plant virus epidemiology. Blackwell Sci. Publ., Oxford, London 1983.
37 Schmelzer, K., Untersuchungen an Viren der Zier- und Wildgehölze. 3. Mitteilung: Virosen an *Robinia, Caryopteris, Ptelea* und anderen Gattungen. Phytopath. Z. *46* (1963) 235–268.
38 Schmelzer, K., Untersuchungen an Viren der Zier- und Wildgehölze. 5. Mitteilung: Virosen an *Populus* und *Sambucus*. Phytopath. Z. *55* (1966) 317–351.
39 Schmelzer, K., Das Ulmenscheckungs-Virus. Phytopath. Z. *64* (1969) 39–67.
40 Schmelzer, K., Das Kirschenblattroll-Virus (cherry leaf-roll virus) aus der Birke (*Betula pendula* Roth.). Z. Bakt., 2. Abt. *127* (1972) 10–12.
41 Schmelzer, K., Nachweis der Verwandtschaft zwischen Herkünften des Kirschenblattroll-Virus (cherry leaf-roll virus) und dem Ulmenmosaik-Virus (elm mosaic virus). Z. Bakt., 2. Abt. *127* (1972) 140–144.
42 Schmelzer, K., Schmidt, H.E., and Schmidt, H.B., Viruskrankheiten und virusverdächtige Erscheinungen an Forstgehölzen. Arch. Forstwesen *15* (1966) 107–120.
43 Schuiling, M., Nienhaus, F., and Kaiza, D.A., The syndrome in coconut palms affected by a lethal disease in Tanzania. Z. PflKrankh. PflSchutz *88* (1981) 665–677.
44 Smith, K.M., Plant Viruses, 6th edn. Chapman & Hall, London 1977.
45 Varney, E.H., and Moore, J.D., Strain of tomato ringspot virus from American elm. Phytopathology *42* (1952) 476–477.
46 Wilson, C.L., Seliskar, C.E., and Krause, C.R., Mycoplasmalike bodies associated with elm phloem necrosis. Phytopathology *62* (1972) 140–143.
47 Yarwood, C.E., and Hecht-Poinar, E., A virus resembling tobacco mosaic virus in oak. Phytopathology *60* (1970) 1320.

0014-4754/85/050597-07$1.50 + 0.20/0

Short Communications

Electron diffraction of the metallic elements in the pineal organ of a freshwater fish, *Mystus vittatus* (Bloch.)

D.K. Srivastava[1], S.S. Khanna, V.M.S. Sriwastwa and R. Kumar[1]

Department of Zoology, K.N. Govt. Postgraduate College, Gyanpur-221304 (India), 10 January 1984

Summary. By electron diffraction pattern the presence of metallic elements, particularly chromium-nickel, chromium phosphide, copper, aluminum-copper and zinc has been shown in the pineal organ of a freshwater teleost, *M. vittatus*. It is likely that their occurrence within the pineal is due to binding with the neurosecretory material fractions/ligands.
Key words. Mystus vittatus; pineal organ; electron diffraction; metallic elements.

The ultrastructure of the teleostean pineal organ has been extensively studied, but the existence of metallic components in the pineal organ of fish has not been investigated so far. There are, however, reports of several investigations where metallic elements were discovered in mammalian pineals [2–8], which motivated the present study.

Over 100 adult *M. vittatus,* which were procured from local ponds at and around Gyanpur (India) were sacrificed in the present study. The pineal organ was carefully taken out with the help of the binocular dissecting microscope (× 20). A 2% glutaraldehyde and 1.3% paraformaldehyde solution[9] in 0.1 M cacodylate buffer (pH 7.2) was used as fixative at 4°C. Quickly-dissected pineal organs were left in fixative for 1.5 h then washed in 0.1 M cacodylate buffer containing 7% sucrose solution. All pineal specimens were post fixed in ice-cold 0.5% osmium tetraoxide solution in the same buffer for 2 h. The fixed pineal was rinsed in four changes of ice-cold double distilled water for 1 h and dehydrated in a graded series of ethanols. After passing through acetone, the whole pineal sac was used as a thin flake and examined with a Philips EM-200 Electron Microscope under transmission by employing the diffraction contrast images (DCI) and selected area diffraction (SAD) modes. Detailed investigation leading to identification of crystalline phases was done by calculating the d-spacing of the diffraction phases through a camera constant by formula: $d = \frac{\text{camera constant}}{r}$ (where d and r denote interplaner spacing and distance of the diffraction lines or spots from the center of transmitted beam position respectively). This constant was obtained by employing spec pure silver (99.999%) thin film as the standard material. The structural data from the ASTM index card were collected and compared against the data calculated from the diffraction experiments. The interplanar d-spacings were also checked and compared.

The DCI mode often revealed the presence of agglomerate which appeared to have a crystalline metallic character. A representative example of this is shown in figure 1. The SAD mode was then utilized to obtain a diffraction pattern (DP) of these agglomerates, which invariably revealed the presence of crystalline components represented by sharp Bragg diffraction rings and/or spots. DP from the randomly oriented tiny agglomerates gave the ring pattern (figs 2–5) and regions of large agglomerates (fig.6) exhibited a single crystal (see figs 7 and 8); the figures show typical examples. The most dominant metallic elements found in the fish pineal were chromium-nickel and chromium-phosphide. The next most often encountered element corresponded to copper. In other cases, as well as these metallic elements others were found, which were identified as

Experientia 41 (1985), Birkhäuser Verlag, CH-4010 Basel/Switzerland

aluminum-copper and zinc. These results are depicted in the table. The existence of copper, zinc and chromium in the pineal organ of *M. vittatus* was verified in a scanning microscope employing EDAX analysis. This supports the observations made by transmission electron microscopy.

It is considered that inorganic components exist as functional constituents within all living cells[10]. In investigations involving the studies of mammalian pineals, the presence of calcium and magnesium[2,7], osmiophilic granules[3,4], copper, mangnese and

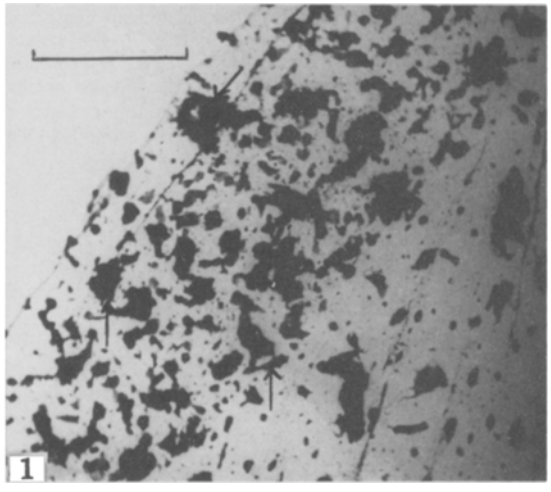

Figure 1. Electron microphotograph reveals the agglomerate (arrows) of tiny crystals in the pineal organ of *M. vittatus* (Bloch.), ×3750 (scale bar = 1 μm).

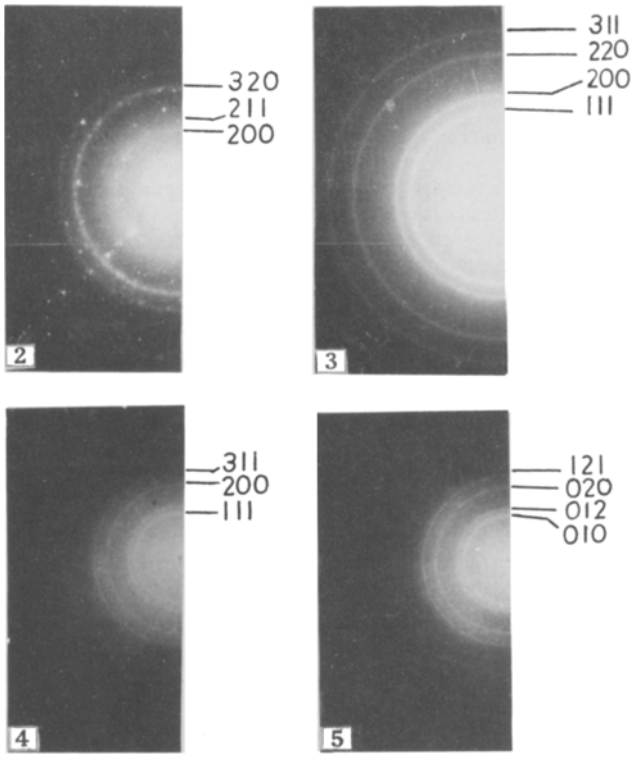

Figure 2. Electron diffraction pattern of pineal organ of *M. vittatus* showing Bragg's rings of chromium-nickel. Figure 3. Electron diffraction pattern of the pineal organ of *M. vittatus* indicating Bragg's rings of chromium-phosphide. Figure 4. Microphotograph shows the electron diffraction pattern of copper in the pineal sac of *M. vittatus*. Figure 5. Bragg's rings of aluminum-copper shown by employing electron diffraction techniques in the pineal sac of *M. vittatus*.

Showing indices of the most intense reflections corresponding to the d-values of identified metallic elements in the pineal organ of *Mystus vittatus* (Bloch.)

Identified metallic elements	Number of specimens examined	Indices of the most intense reflection	d-values (Å) Standard (ASTM*)	calculated (EXPTL**) SE ± 0.05 Å)	Electron diffraction pattern
Chromium-nickel	30	211	1.870	1.814	Powder
Chromium-phosphide	30	111	2.378	2.450	Powder
Copper	24	111	2.088	2.112	Powder
Aluminium-copper	24	010	3.580	3.586	Powder
Zinc	20	10.0	2.308	2.261	Single crystal

* American Society for Testing Materials. ** Data calculated from the diffraction experiment. SE denotes experimental error limit.

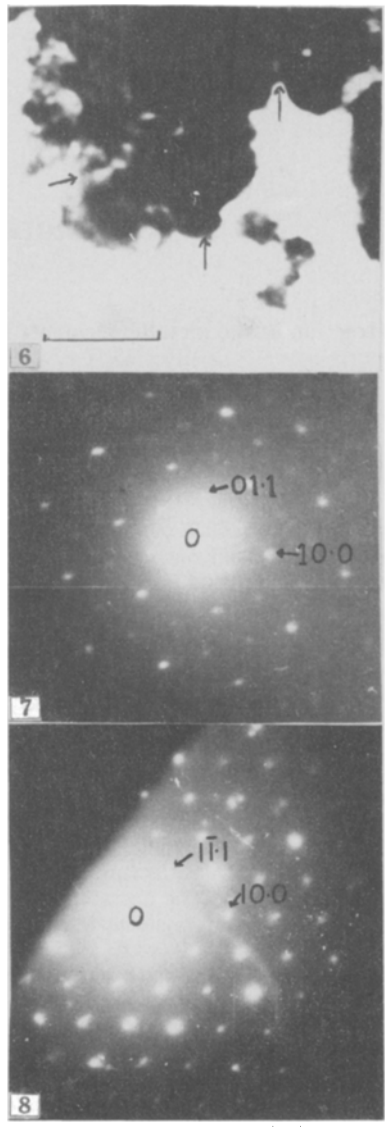

Figure 6. Electron microphotograph exhibiting the agglomerate (arrows) of individual crystalline forms in the pineal sac of *M. vittatus*, × 3750 (scale bar = 1 μm).

Figures 7 and 8. Bragg's spots indicate the presence of single crystal pattern of zinc in the pineal sac of *M. vittatus* by employing electron diffraction pattern.

zinc[5] and calcospherulites[6] as quoted by Relkin[8] have been recognized. Quay[7] also stated that molybdenum, iodine, cobalt, aluminum, barium, chromium, titanium, silver, nickel, mercury, strontium and lead are worthy of analysis in the pineal organ. The results of the present analysis revealed that the pineal organ of the freshwater teleost, *M. vittatus* definitely contains chromium-nickel, chromium-phosphide, copper, aluminum-copper and zinc.

Histochemical studies suggest a variable presence of carbohydrates, proteins, lipids and mucoid substances in pineal organs from the same fish, containing many amino ($-NH_2$), carboxyl ($-COOH$), hydroxyl ($-OH$), phosphonyl ($-PO_3H_2$), sulfhydryl ($-SH$) and thiol groups[11]. As in most of the mammalian species it is possible that these histochemical fractions/ligands of neurosecretory activity within the fish pineal provide binding sites for these inorganic constituents. It is expected that the results of the present investigation will further induce pinealogists to elucidate the probable role of these elements in the metabolic fate of the pineal complex.

1 The technical assistance of O. N. Srivastava and financial assistance of CSIR, India, are gratefully acknowledged.
2 Angervall, L., Berger, S., and Rockert, H., Acta path. microbiol. scand. *44* (1958) 113.
3 DeMartino, C., DeLuca, F., Paluello, F. M., Tonietti, G., and Orci, L., Experientia *19* (1963) 639.
4 Perrelet, A., Orci, L., and Rouiller, C., Experientia *24* (1968) 1047.
5 Wong, P. Y., and Fritze, K., J. Neurochem. *16* (1969) 1231.
6 Mabie, C. P., and Wallace, B. M., Cell Tissue Res. *16* (1974) 59.
7 Quay, W. B., in: Pineal Chemistry. Ed. N. Kugelmass. Charles C. Thomas, Springfield, Illinois 1974.
8 Relkin, R., in: The Pineal. Churchill Livingstone, Eden Press 1976.
9 Karnovsky, M. J., and Roots, L., J. Histochem. Cytochem. *12* (1965) 219.
10 Morston, H. R., Physiol. Rev. *32* (1952) 66.
11 Khanna, S. S., Sriwastwa, V. M. S., Srivastava, D. K., and Kumar, R., Adv. biol. Res. *1* (1982) 32.

0014-4754/85/050603-03$1.50 + 0.20/0

Effects of carotid sinus nerve stimulation on respiratory sinus arrhythmia and respiratory blood pressure waves of the dog

H. Warzel and H.-U. Eckhardt

Institut für Physiologie, Medizinische Akademie Magdeburg, Leipziger Strasse 44, DDR-3090 Magdeburg (German Democratic Republic), 15 December 1983

Summary. The effect on the amplitudes of RSA and RBPW of the time of the stimulus in the cardiac cycle, and also of continuous stimulation were studied. When the stimulus train was applied near peak systole the amplitudes of RSA and RBPW decreased. Stimulation in late systole increased both RSA and RBPW. Continuous stimulation did not exert any effects on RSA and RBPW.
Key words. Carotid sinus nerve stimulation (CSNS), R wave-triggered; respiratory sinus arrhythmia (RSA); respiratory blood pressure waves (RBPW); cardio-respiratory coordination.

The heart is under the continuous but changing influence of efferent sympathetic and parasympathetic activity[1]. In addition to various forms of peripheral and central mechanisms, this efferent activity is very efficiently influenced by baro- and chemoreceptors[2] as well as by respiratory rhythm[3,4]. The central interactions of these input into the 'common brain stem system'[5] affect sympathetic and parasympathetic activity usually in opposite directions. Consequences of such interaction are the respiratory cycle-related sensitivity of the baroreceptor reflex[4,6-8], the RSA[3,4,9,10] and the RBPW[3,8,11,12]. The effectiveness of the baroreceptor reflex is dependent on the position of the stimulus in the cardiac cycle, too[13,14]. Stimulation of the medullary pressor[15], the depressor[16] areas, the aortic depressor[17] and the carotid sinus nerve[18] produces a very pronounced effect on the efferent sympathetic activity in response to stimuli applied in the early systole.

The R wave-triggered CSNS during this cardiac phase causes the RBPW to vanish[19].

To date, however, no systematic studies have been carried out on RSA and RBPW responses with respect to stimulus position in the cardiac cycle. Therefore, we studied the influence of CSNS at various time intervals after the R wave of the ECG on the amplitudes of RSA and RBPW. It was the aim of this study to obtain new findings on interactions and interconnections between the respiratory and rapidly-reacting cardiovascular control systems.

Material and methods. Experiments were done on 13 adult spontaneously breathing dogs (11–34 kg) of either sex, anesthetized with ethyl urethane (375 mg/kg, i.m.) following premedication with morphine sulfate (15 mg/kg). Supplementary urethane was given by i.v. drip at a rate of 62.5 mg/kg/h. The carotid sinus nerves (CSN) were identified by recording their pulsatile nerve activity, and placed on bipolar platinum electrodes in a pool of mineral oil for stimulation.

The intact CSN was stimulated with short trains of impulses given at various times in the cardiac cycle. Each train consisted of five square-wave impulses inserted 0–210 ms after the R wave of the ECG. The impulse duration was 0.5–1 ms and the impulse spacing 25 ms. Identical parameters were used for continuous stimulation. The stimulating current was adjusted in such a way that the CSN depressor response would be 2 kPa (usually 0.1–3 mA). Current values and the impulse form were monitored on a cathode-ray oscilloscope. Breathing was enhanced only to a minor extent if at all, by the above stimulus parameters. Each stimulation series for the various delay settings lasted about 2 min and was followed by a recovery period of 2 min.

Polyethylene catheters were inserted into the femoral artery to record arterial pressure, and into the femoral vein for administration of drugs.

Arterial pressure, ECG and the beat-by-beat heart rate were recorded by means of a multichannel oscillographic recorder. The ECG potentials were used to operate a linear instantaneous rate meter, the function of which was to produce an output voltage whose amplitude was at all times inversely proportional to the time interval between the last two input impulses, i.e. proportional to the instantaneous rate (fig. 1). To evaluate the relative influence of the respiration on heart rate and blood pressure, the indexes $\triangle RSA = RSA_{st} - RSA_o$ and $\triangle RBPW = RBPW_{st} - RBPW_o$ (o = prior to, st = during stimulation) where $RSA = HR_{MAX} - HR_{MIN}$ and $RBPW = BP_{MAX} - BP_{MIN}$ (MAX = high, and MIN = low value during respiratory cycle), were calculated.

Statistical evaluation of the findings was made by use of the concordance coefficient (Kendall) with a given $p < 0.001$.